

Supporting Information

Aqueous Al–PbO₂ Battery with pH-Gradient Engineering Surpasses 3.5 V

*Yingyi Zeng, Zhiwen Lu, Kai Chen, Zhenhai Wen **

^a State Key Laboratory of Structural Chemistry, and Fujian Provincial Key Laboratory of Materials and Techniques toward Hydrogen Energy, Fujian Institute of Research on the Structure of Matter, Chinese Academy of Sciences, Fuzhou, Fujian, 350002, China.

^b College of Chemistry and Materials Science, Fujian Normal University, Fuzhou, 350007, China.

^c Fujian College, University of Chinese Academy of Sciences, Fuzhou, Fujian, 350002, China.

Corresponding Author

Zhenhai Wen – E-mail: wen@fjirsm.ac.cn.

Experimental Section

Materials

All chemicals are of analytical grade and used without further purification. HNO_3 and ethanol were purchased from Sinopharm. sodium dodecyl sulfate was purchased from Aladdin. Titanium mesh was purchased from Kunshan Guangjiayuan New Material Co., Ltd. The proton membrane was purchased from Dupont. Commercial Pt/C (20 wt%) was purchased from Shanghai Hesen Electric Co., Ltd. Commercial PbO_2/Ti electrodes were purchased from Suzhou Schulte Industrial Technology Co., Ltd.

Material synthesis

Synthesis of PbO_2/Ti electrode

The PbO_2/Ti electrode was synthesized via an electrochemical deposition method. Specifically, 0.16 mol L^{-1} lead nitrate $\text{Pb}(\text{NO}_3)_2$ and 0.5 g L^{-1} sodium dodecyl sulfate (SDS) were dissolved in a mixture of 500 μL dilute nitric acid and 80 mL deionized water. The resulting acidic solution was stirred magnetically and maintained at 65 °C in a thermostatic water bath to ensure complete dissolution, forming the deposition bath.

The electrodeposition was carried out in a 100 mL beaker under continuous magnetic stirring and constant temperature (65 °C). A titanium mesh (10 mm × 20 mm) was used as the working electrode (anode), and a commercial Ru–Ir/Ti electrode of identical dimensions served as the counter electrode (cathode). The distance between the electrodes was maintained at 1 cm. A constant current density of 250 mA cm^{-2} was applied for 3 hours to fabricate the PbO_2/Ti electrode with a uniform and compact surface morphology.

Material characterization

X-ray powder diffraction (XRD) was performed on a (Miniflex 600, Rigaku) powder x-ray diffractometer with $\text{Cu K}\alpha$ radiation ($\lambda = 1.54178 \text{ \AA}$, 40 kV, 15 mA) at a scan rate of 10 °/min. The microscopic morphology and structure of the samples were

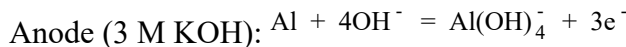
investigated by scanning electron microscopy (SEM, JSM6700-F) and transmission electron microscopy (TEM, TECNAI G2 F20). In situ Raman spectra were acquired with a 532 nm laser on a LabRAM HR. The x-ray photoelectron spectra (XPS) were obtained on an XPS spectrometer Thermo Scientific K-Alpha using Al K α rays ($h\nu=1486.66$ eV) as the excitation source.

Electrochemical characterization

All the galvanostatic charge-discharge (GCD) and cyclic voltammetry (CV) curves were tested on the electrochemical workstation (CHI E760) including the two electrode Al-PbO₂ hybrid battery and the three electrode systems containing PbO₂ as working electrode, reference electrode of silver chloride and counter electrode of platinum net in acid or alkaline electrolyte. The cyclic stability testing Al-PbO₂ hybrid battery were performed on land battery test system (LAND CT2001A). The charge time of GCD was decided by duration of charging plateau to avoid the state of overpotential and HER for maintaining the Coulombic efficiency over 90%.

Theoretical electrochemical properties of Hybrid Acid-Alkaline Al-PbO₂ Battery

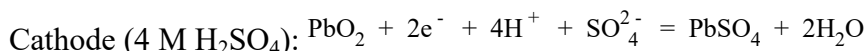
Discharge process:



$$E_a = \frac{E_{\text{Al}(\text{OH})_4^-}^\theta - 2.303 \frac{RT}{2F} \log \left[(\alpha_{\text{OH}^-})^4 \right]}{\text{Al}} = -2.328 \text{ V} - 0.0789 * \log (\alpha_{\text{OH}^-}) = -2.365 \text{ V}$$

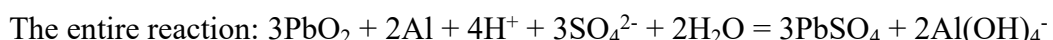
$$E_{\text{Al}(\text{OH})_4^-}^\theta = -2.328 \text{ V vs. SHE}$$

$$\left(\frac{\text{Al}(\text{OH})_4^-}{\text{Al}} \right) \quad (\text{Eq. 1})$$



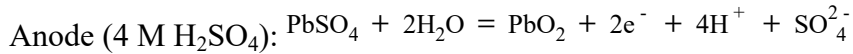
$$E_c = \frac{E_{\text{PbO}_2}^\theta - 2.303 \frac{RT}{nF} \log \left[\frac{\alpha_{\text{PbSO}_4} \times \alpha_{\text{H}_2\text{O}}^2}{\alpha_{\text{PbO}_2} \times \alpha_{\text{H}^+}^4 \times \alpha_{\text{SO}_4^{2-}}} \right]}{\text{PbSO}_4} = 1.6711 \text{ V} + 0.1478 * \log (\alpha_{\text{H}^+}) = 1.804 \text{ V}$$

$$\left(E_{\text{PbO}_2}^\theta = 1.6711 \text{ V vs. SHE} \right) \quad (\text{Eq. 2})$$



$$V_{\text{cell}} = E_c - E_a = 4.169 \text{ V} \quad (\text{Eq. 3})$$

Charge process:



$$E_a = E_{\frac{\text{PbO}_2}{\text{PbSO}_4}}^\theta - 2.303 \frac{RT}{nF} \log \left[\frac{\alpha_{\text{PbSO}_4} \times \alpha_{\text{H}_2\text{O}}^2}{\alpha_{\text{PbO}_2} \times \alpha_{\text{H}^+}^4 \times \alpha_{\text{SO}_4^{2-}}} \right] = 1.6711 \text{ V} + 0.1478 * \log(\alpha_{\text{H}^+}) 1.804 \text{ V}$$

$$\left(E_{\frac{\text{PbO}_2}{\text{PbSO}_4}}^\theta = 1.6711 \text{ V vs. SHE} \right) \quad (\text{Eq. 4})$$



$$E_c = E_{\frac{\text{H}^+}{\text{H}_2}}^\theta - 2.303 \frac{RT}{2F} \log \left[\frac{\alpha_{\text{H}_2}}{(\alpha_{\text{H}^+})^2} \right] = 0 \text{ V} + 0.059 * \log(\alpha_{\text{H}^+}) = 0.035 \text{ V}$$

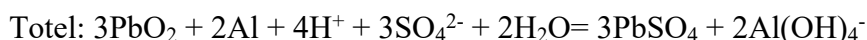
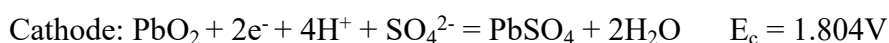
$$\left(E_{\frac{\text{H}^+}{\text{H}_2}}^\theta = 0 \text{ V vs. SHE} \right) \quad (\text{Eq. 5})$$

$$V_{\text{cell}} = E_c - E_a = -1.751 \text{ V} \quad (\text{Eq. 6})$$

Notes: R is the gas constant ($8.314 \text{ J mol}^{-1} \text{ K}^{-1}$), α is the corresponding activity, F is the Faraday constant, 96485 C mol^{-1} , and T is 298.15 K .

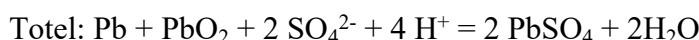
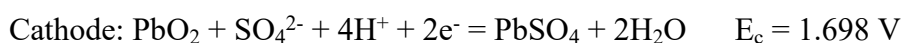
From the comparison of the following chemical equations, it can be seen that the voltage of the Al-PbO₂ battery is higher than that of the conventional lead-acid battery.

Al-PbO₂ battery:



$$E_{\text{cell}} = E_c - E_a = 4.169 \text{ V}$$

Conventional lead-acid batteries:



$$E_{\text{cell}} = E_c - E_a = 2.054 \text{ V}$$

Faraday efficiency calculation

In order to monitor the H₂ production, we recorded the volume (V) of hydrogen produced every 10 min at a current density of 5, 10, 15, 20, and 25 mA cm⁻² using the drainage method. The molarity of H₂ (n) can be expressed by the following equation:

$$n = \frac{V}{V_m}$$

Where V_m is the molar volume of the gas (24.5 L/mol)

The theoretical H₂ volume can be calculated by the following equation:

$$n_{\text{theo}} = \frac{Q}{N * F} = \frac{I * t}{N * F}$$

Where Q is the charge transfer, N is the number of electrons transferred to produce each H₂ molecule (N = 2), F is the Faraday constant (96,500 C mol⁻¹), I is the discharge current (mA), and t is the operating time (s).

Therefore, the Faraday efficiency (FE) of H₂ can be calculated as follows:

$$FE(\%) = \frac{n}{n_{\text{theo}}} \times 100\%$$

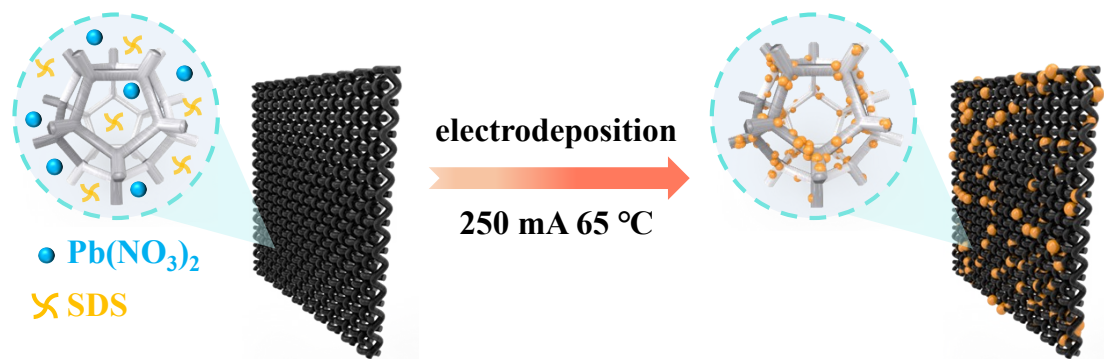


Figure. S1 Schematic of the synthesis procedures for PbO_2/Ti electrode.

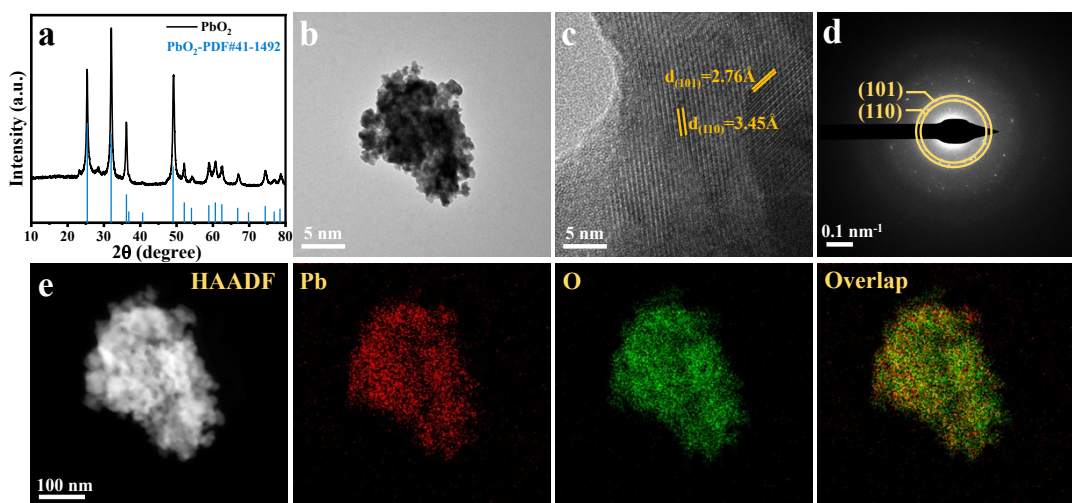


Figure. S2 a) XRD pattern of PbO_2/Ti . b-c) HRTEM image of PbO_2 . d) SAED pattern of PbO_2 . e) HAADF-STEM image of a PbO_2 and its EDS elemental maps of Pb and O.

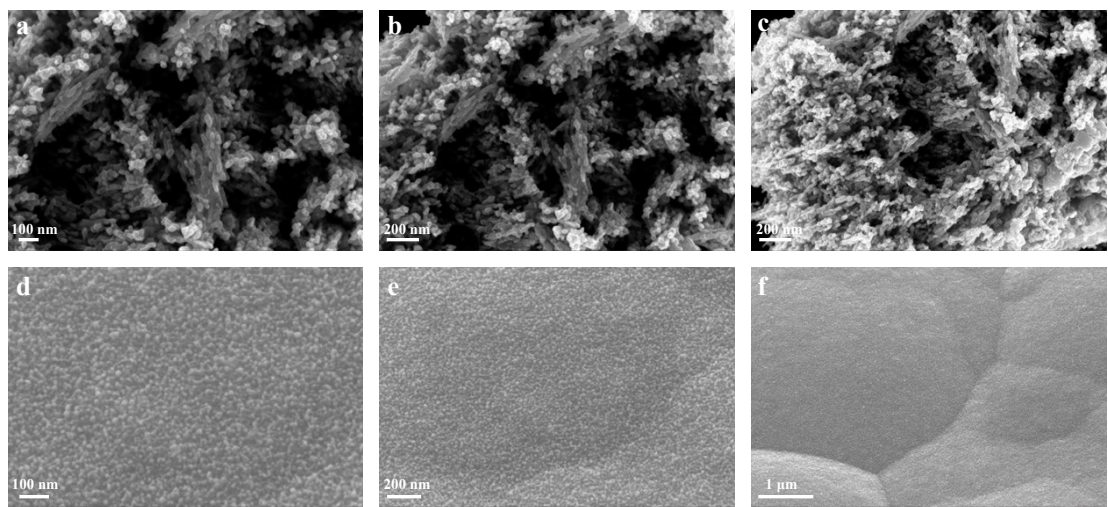


Figure. S3 a-c) PbO₂ SEM images at different scales. d-f) PbO₂/Ti SEM images at different scales.

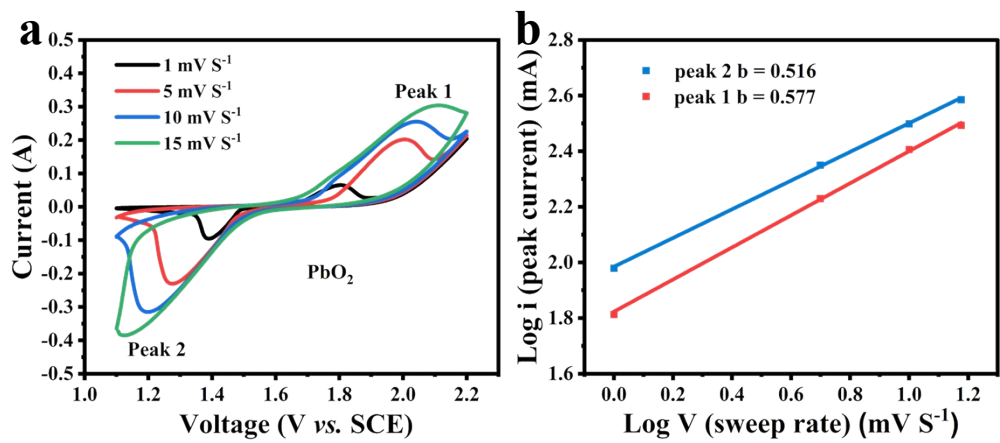


Figure. S4 a) Cyclic voltammetry (CV) curves at different scan rates. b) plot of rate law ($\log i$ vs. $\log v$) for the two redox couples.

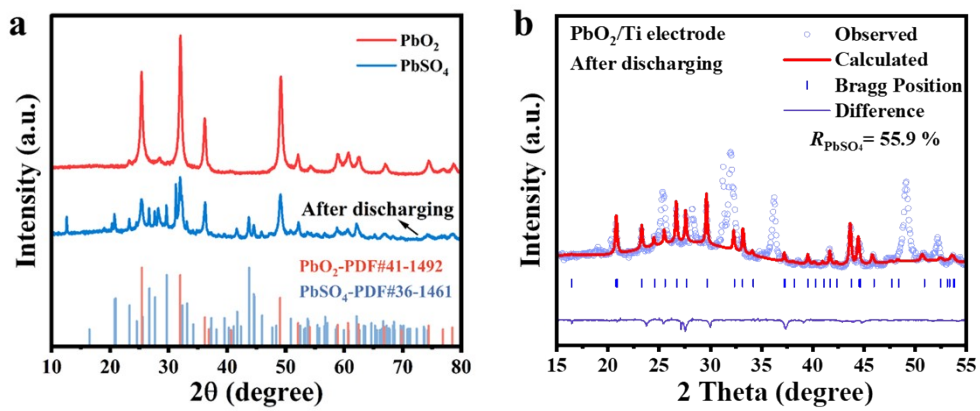


Figure. S5 a) XRD pattern of PbO_2 /Ti electrodes before and after discharging. b) Quantitative rietveld refinement analysis.

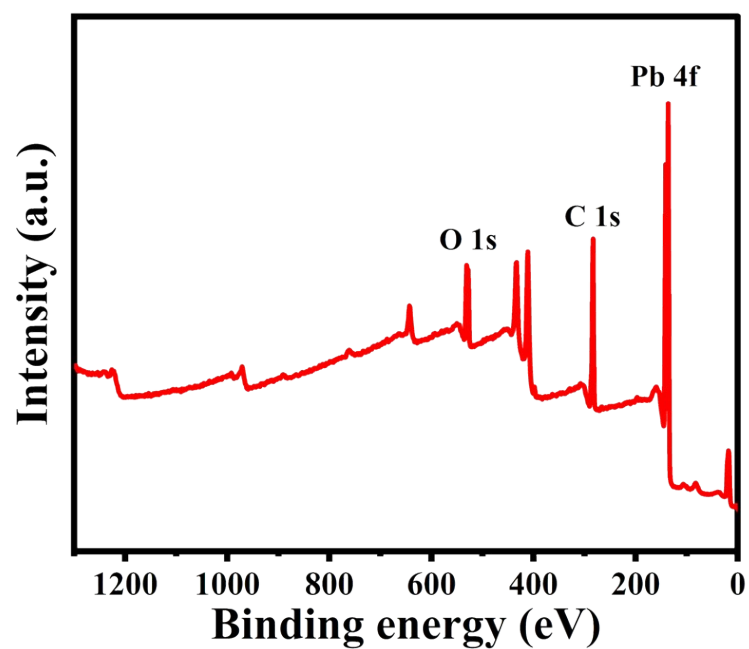


Figure. S6 The survey XPS spectrum of PbO_2/Ti electrodes.

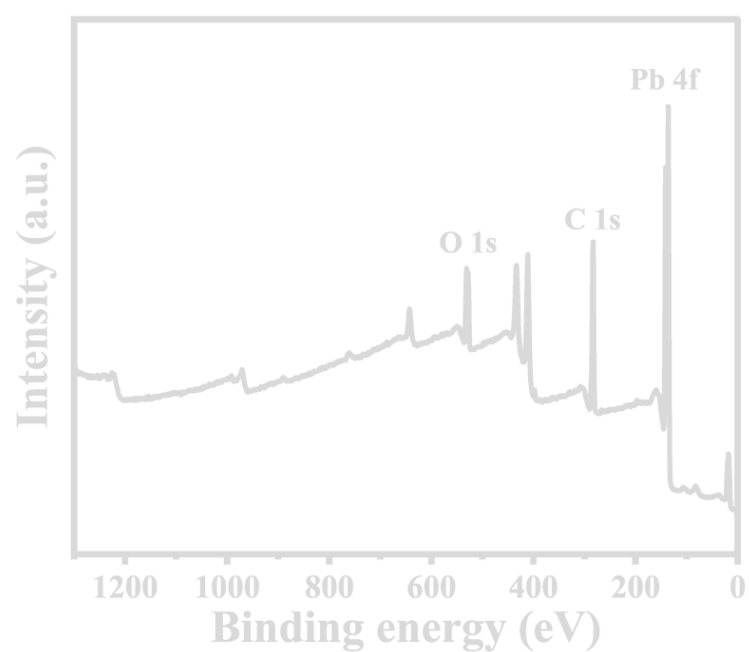


Figure. S7 The survey XPS spectrum of PbO_2/Ti electrodes after discharging.

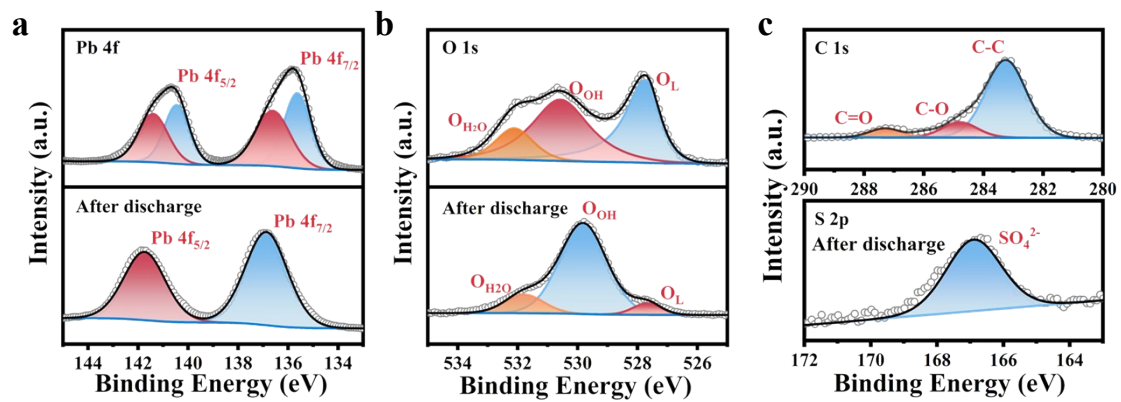


Figure. S8 High-resolution XPS spectra of PbO₂/Ti electrodes. a) Pb 4f. b) O 1s. c) C 1s and S 2p.

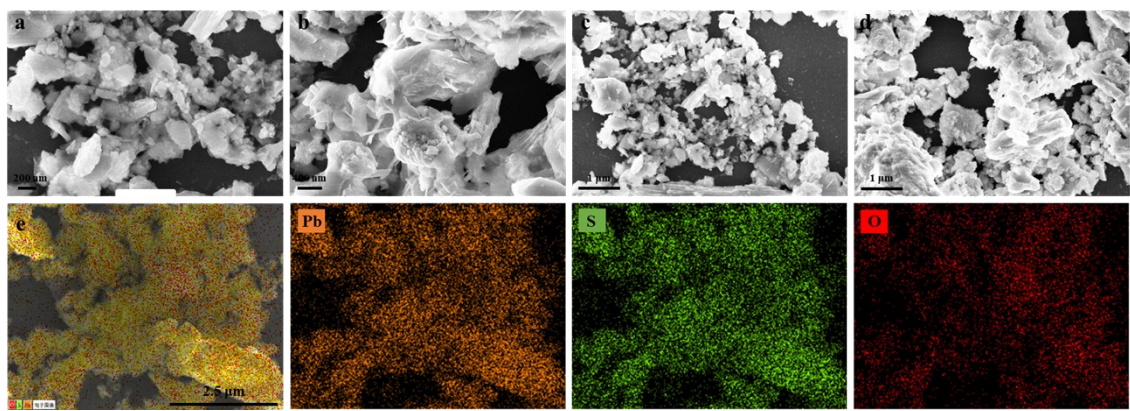


Figure. S9 (a-d) SEM and e) EDS of the electrode after discharging.

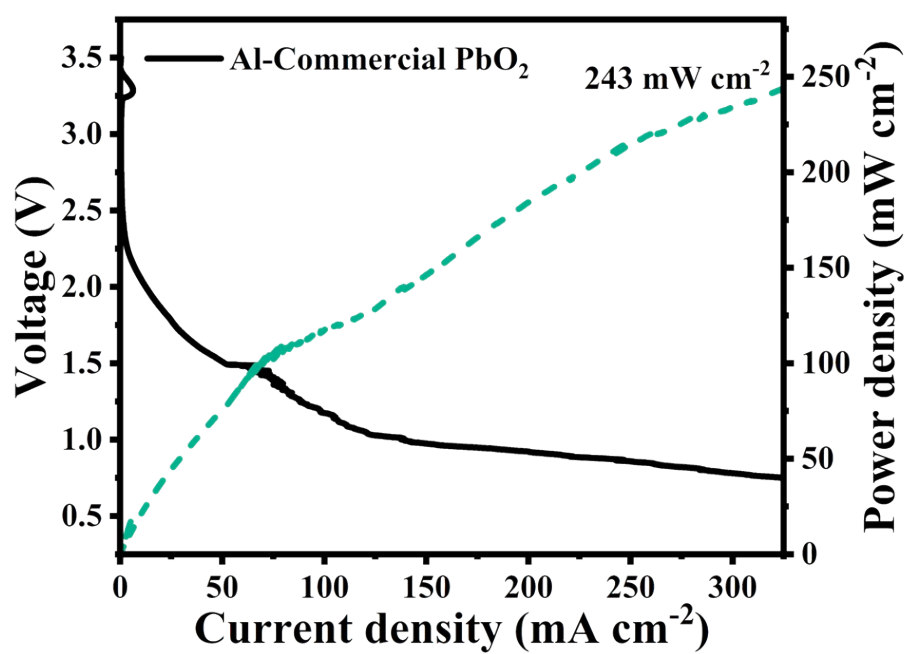


Figure. S10 Discharging polarization curves and corresponding power density curves of Al-Commercial PbO_2 hybrid battery.

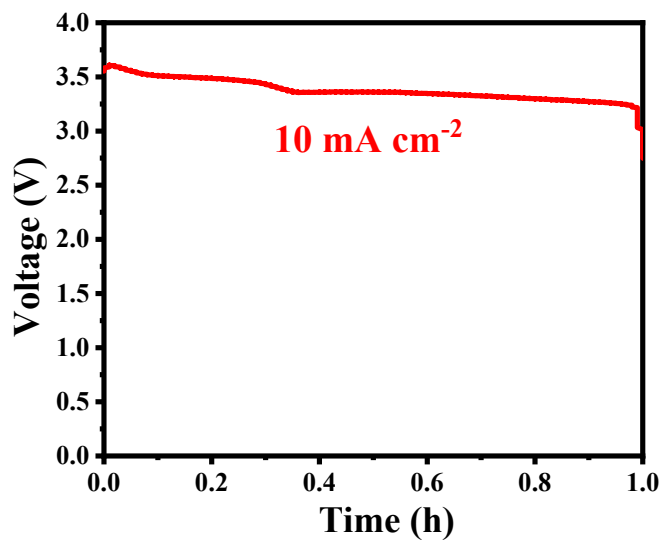


Figure. S11 The discharge curve at a current density of 10 mA cm^{-2} .

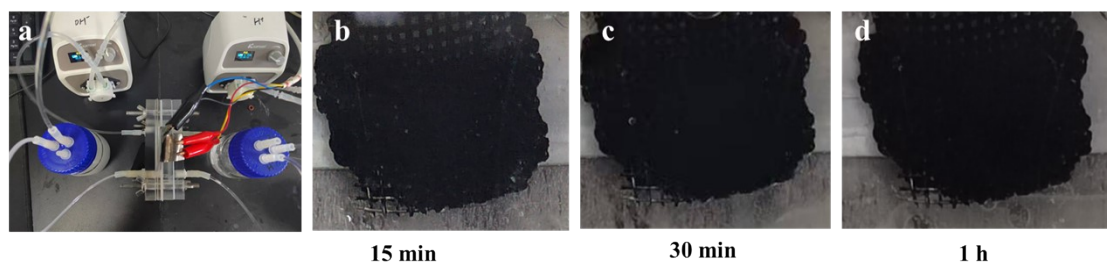


Figure. S12 Changes on the electrode surface during the discharge process. a) Battery physical diagram. b) Discharge for 15 minutes. c) Discharge for 30 minutes. d) Discharge for 60 minutes.

Caption: As shown in the figure S12, no visible gas bubbles were observed throughout the discharge process. This provides clear experimental evidence that HER was effectively suppressed under our operational conditions.

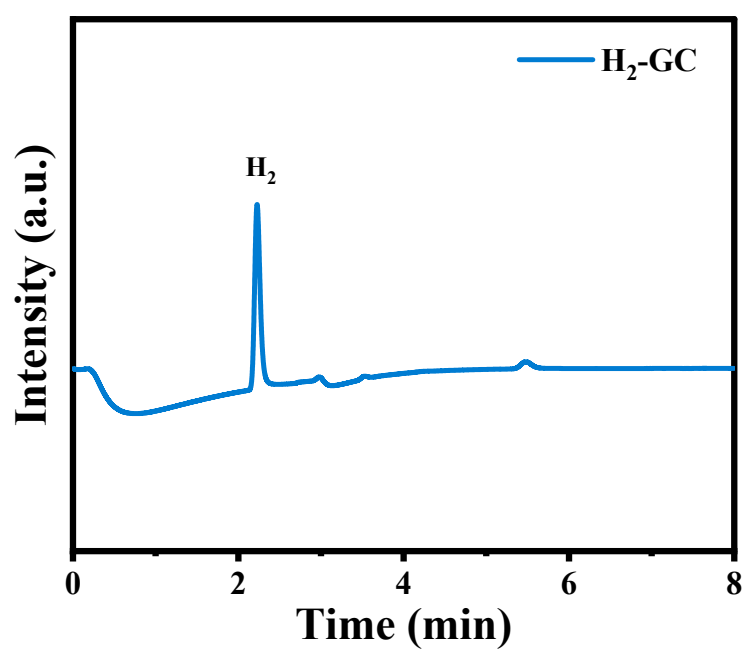


Figure. S13 The gas chromatography curve of H₂ during the charging process.

Caption: Gas chromatography analysis of the gas evolved during the charging process, confirming the identity of the gas as hydrogen (H₂) by comparison with a standard.

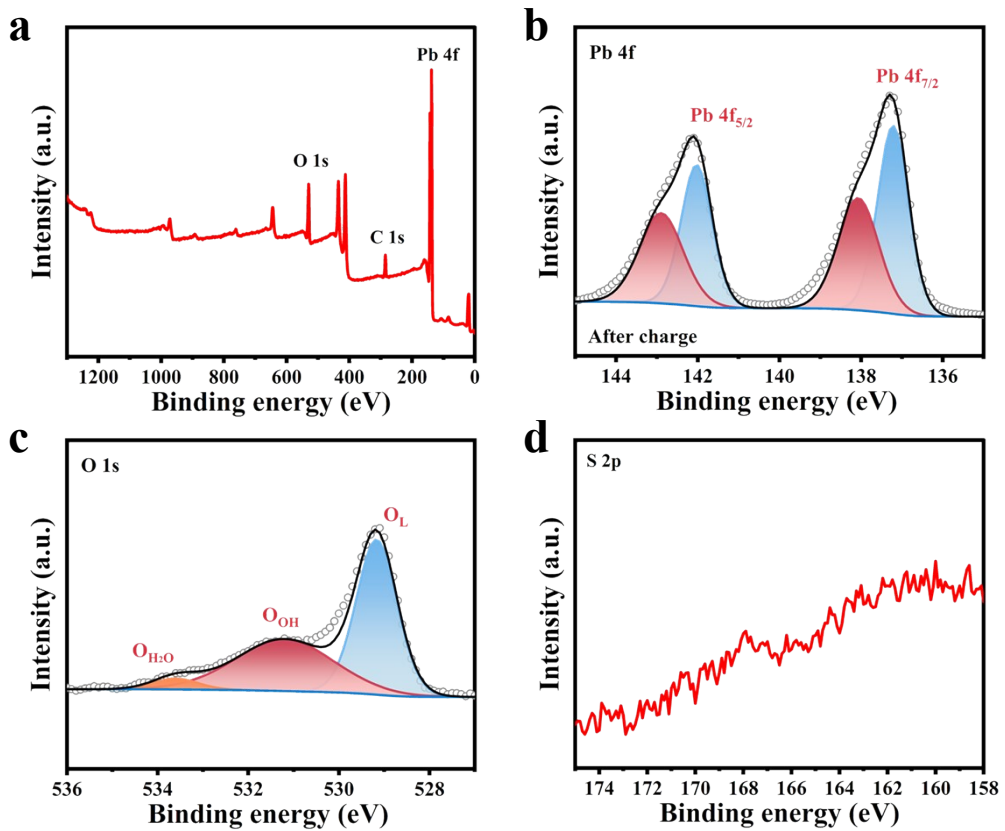


Figure. S14 High-resolution XPS spectra of after charge PbO₂/Ti electrodes. a) The survey XPS spectrum of PbO₂/Ti electrodes after charging. b) Pb 4f. c) O 1s. d) S 2p.